FEBS Letters 586 (2012) 640–645

journal homepage: www.FEBSLetters.org

Review

Reconstitution of respiratory oxidases in membrane nanodiscs for investigation of proton-coupled electron transfer

Linda Näsvik Öjemyr [a], Christoph von Ballmoos [a], Robert B. Gennis [b], Stephen G. Sligar [c], Peter Brzezinski [a,*]

[a] Department of Biochemistry and Biophysics, The Arrhenius Laboratories for Natural Sciences, Stockholm University, SE-106 91 Stockholm, Sweden
[b] Department of Biochemistry, University of Illinois at Urbana–Champaign, Urbana, IL 61801, United States
[c] Department of Chemistry, University of Illinois at Urbana–Champaign, Urbana, IL 61801, United States

ARTICLE INFO

Article history:
Received 25 October 2011
Revised 19 December 2011
Accepted 21 December 2011
Available online 29 December 2011

Edited by Miguel Teixeira and Ricardo O. Louro Ready

Keywords:
Cytochrome *c* oxidase
Cytochrome aa_3
Cytochrome ba_3
Membrane protein
Lipid
Energy transduction

ABSTRACT

The function of membrane-bound transporters is commonly affected by the milieu of the hydrophobic, membrane-spanning part of the transmembrane protein. Consequently, functional studies of these proteins often involve incorporation into a native-like bilayer where the lipid components of the membrane can be controlled. The classical approach is to reconstitute the purified protein into liposomes. Even though the use of such liposomes is essential for studies of transmembrane transport processes in general, functional studies of the transporters themselves in liposomes suffer from several disadvantages. For example, transmembrane proteins can adopt two different orientations when reconstituted into liposomes, and one of these populations may be inaccessible to ligands, to changes in pH or ion concentration in the external solution. Furthermore, optical studies of proteins reconstituted in liposomes suffer from significant light scattering, which diminishes the signal-to-noise value of the measurements. One attractive approach to circumvent these problems is to use nanodiscs, which are phospholipid bilayers encircled by a stabilizing amphipathic helical membrane scaffold protein. These membrane nanodiscs are stable, soluble in aqueous solution without detergent and do not scatter light significantly. In the present study, we have developed a protocol for reconstitution of the aa_3- and ba_3-type cytochrome *c* oxidases into nanodiscs. Furthermore, we studied proton-coupled electron-transfer reactions in these enzymes with microsecond time resolution. The data show that the nanodisc membrane environment accelerates proton uptake in both oxidases.

1. Introduction

One role of biological membranes is to define the boundary of cells and organelles. Intrinsic membrane proteins that span across these membranes are involved in fundamental processes such as signaling, energy conversion, motility and transport. A challenge associated with studies of these membrane proteins is to mimic the membrane environment, which is necessary to make the proteins soluble in water. The choice of this membrane mimetic is an important parameter because the structure and function of membrane proteins is often dependent on specific interactions between the membrane lipids and the protein [1–3]. Approaches to study purified membrane proteins in aqueous solutions include, for example, the use of detergents [4]. However, many membrane proteins are unstable and/or lose their function in detergent solution. In these cases, it may be more attractive to use liposomes, composed of different, well defined lipids, both native and synthetic, simulating a natural environment of the protein. Because such liposomes have an inner compartment that is sealed from the surrounding outside bulk solution, they allow studies of ion or molecule transport across the membrane. However, in many cases, studies of proteoliposomes suffer from significant drawbacks. For example, liposomes scatter light, which diminishes the signal-to-noise value in optical measurements. Furthermore, commonly, transmembrane proteins reconstituted in liposomes are only partially oriented such that there are two protein populations sensing different solvent phases. Similarly, a non-uniform enzyme orientation may influence studies in which non membrane-permeable interaction partners are added. In many cases, functional studies of membrane-bound proteins (including those that are involved in transmembrane transport) do not require sealed liposomes, an open system where both sides of the membrane protein are

Abbreviations: MSP, membrane scaffold protein; CytcO, cytochrome *c* oxidase; *n*,*p*-side, negative and positive sides of the membrane, respectively; DDM, *n*-dodecyl β-D-maltoside; PCET, proton-coupled electron transfer

* Corresponding author.
E-mail address: peterb@dbb.su.se (P. Brzezinski).

0014-5793 © 2011 Published by Elsevier B.V. on behalf of the Federation of European Biochemical Societies. Open access under CC BY-NC-ND license.
doi:10.1016/j.febslet.2011.12.023

exposed to identical solvent environments (cf. pH, ionic strength etc.) is an advantage. A recently developed alternative to using liposomes in such cases is the so-called nanodisc technology [5,6]. These discs are planar phospholipid bilayers surrounded by two membrane-scaffold proteins (MSPs), whose amphiphilic helical structure covers the exposed hydrophobic edges of the lipid bilayer. Thus, the membrane proteins can be studied while soluble in aqueous solutions, yet residing in a native-like membrane bilayer environment of well-defined composition. The nanodiscs are more stable than liposomes and their size (Ø ≅ 10–17 nm) and lipid content (120–330 lipids, for empty discs, depending on lipids [6]) renders dramatically less light scattering compared to liposomes (Ø ≅ 30–200 nm, 4–180 × 10^3 lipids), which makes the nanodisc technology ideal for studies of membrane proteins using optical techniques. In addition, the lower lipid-protein ratio in nanodiscs as compared to liposomes is of significant advantage in studies of proton uptake/release reactions because of the buffering capacity of phospholipid head groups.

Here, we have developed a protocol for reconstitution of the membrane-bound proton pump cytochrome *c* oxidase (Cyt*c*O) into nanodiscs composed of soybean lipids using the scaffold protein MSP1E3D1, which yields nanodiscs with a diameter of ∼12 nm [7]. Two different Cyt*c*Os were studied, the aa_3-type Cyt*c*O from *Rhodobacter sphaeroides* [8–10] and the ba_3-type Cyt*c*O from *Thermus thermophilus* [11–13]. These Cyt*c*Os catalyze the reduction of O_2 to H_2O: $O_2 + 4H^+ + 4e^- \rightarrow 2H_2O$ (for review, see [14–19]). Electrons are delivered by a water-soluble cytochrome *c*, which docks at the more positive (*p*) side of the membrane. The primary electron acceptor is a copper center, Cu_A, from which electrons are transferred to a heme group (heme *a* or *b*) and then to the catalytic site composed of heme a_3 and Cu_B, where O_2 binds and becomes reduced. Protons are taken up from the more negative (*n*) side of the membrane and are transferred through specific pathways. The aa_3 oxidase has been shown to use two such pathways denoted by letters D and K, respectively, while the ba_3 Cyt*c*O uses only one pathway that overlaps in space with the K pathway in the aa_3 Cyt*c*O [20,21]. Results from earlier experiments with the aa_3 Cyt*c*O have shown that internal electron transfer to or from the catalytic site, linked to proton uptake or release through the K pathway is sensitive to the membrane environment of the Cyt*c*O [22] (see also [23]). Using the nanodisc technology, we have studied the kinetics, with microsecond time resolution, of these internal electron and proton-transfer reactions.

2. Materials and methods

2.1. Growing and purification of cytochrome c oxidase

The aa_3- and ba_3-Cyt*c*Os were expressed in *R. sphaeroides* and *T. thermophilus*, respectively, and the His-tagged protein was purified using Ni-affinity chromatography as described earlier [24,25].

2.2. Reconstitution of CytcO into nanodiscs

The soybean phosphatidyl choline lipids (type II, Sigma) were washed by diethyl ether extraction and then precipitation using acetone. The lipids were then extensively dried to remove all traces of organic solvents. The washed lipids (final concentration of 40 mg/ml) were then resuspended in 50 mM Tris–HCl pH 7.5 containing 120 mM sodium cholate hydrate (Fluka/Sigma). The sample was sonicated to complete dissolution of the lipids using a tip sonciator (Ultra sonic VCX 130, Chemical Instruments AB, Sweden) for two minutes per ml sample in cycles of 30 s on and 30 s off. Particles from the sonicator tip were removed by centrifugation at 4500×*g* for 20 min. The lipid-cholate mixture was mixed with the MSP1E3D1 protein and aa_3- or ba_3-Cyt*c*O at an approximate molar ratio of 500:10:1 (Lipid:MSP:Cyt*c*O). Buffer was added to keep the cholate and lipid concentrations at 25 mM and 6 mg/ml, respectively. The sample mixture was incubated for one hour at room temperature with occasional gentle shaking. The detergent was then removed using a PD-10 column (GE Healthcare) pre-equilibrated with 50 mM Tris–HCl pH 7.5 and the eluate containing color was collected (the sample was loaded in several fractions, each having a volume of 500–750 μl). For nanodiscs containing fluorescent lipids, soybean lipids were first dissolved in chloroform and mixed with Texas Red (TR) DHPE (Invitrogen) to yield on average one fluorescent lipid per 10 nanodiscs and the solvent was evaporated under a stream of nitrogen before the dry lipid film was dissolved using the same procedure as described above.

2.3. Analysis of CytcO-containing nanodiscs

Samples were concentrated using a protein concentrator tube (100 kDa, Millipore) and centrifuged at 10 000×g for 30 min before injection of a volume of 100 μl onto a Superdex 200 10/300 GL Column (GE Healthcare) equilibrated with 50 mM phosphate buffer at pH 7.5 and 100 mM KCl. After injection, 1 ml fractions were collected at a flow rate 0.25 ml/min. Absorbance spectra at 240–700 nm were recorded for each fraction using a dip probe (Cary 50, Varian). Fractions containing protein were concentrated by a factor of 10 and used for SDS–PAGE (NuPAGE 4–12% Bis–Tris, Invitrogen). The samples containing fluorescent lipids were analyzed in a 96 well plate reader (SpectraMax Gemini EM microplate spectrofluorometer Molecular Devices).

2.4. Preparation of the two-electron reduced aa_3 CytcO and measurements of PCET

For aa_3-Cyt*c*O, the nanodisc sample buffer was exchanged for 100 mM KCl on a PD-10 column and the pH was adjusted to 9.0 before transferring it to an anaerobic cuvette. First, the atmosphere in the cuvette was exchanged to N_2 and subsequently to CO. The reduction state of the enzyme was monitored using a spectrophotometer (Cary 400 Varian) to reach the two-electron reduced state. The cuvette was then transferred to the flash photolysis apparatus, where the CO ligand was dissociated by applying a short laser flash (10 ns, 200 mJ, 532 nm, Nd:YAG Brilliant B, Quantel) and electron transfer was monitored at different single wavelengths. In samples containing detergent-solubilized enzyme solution, *n*-dodecyl β-D-maltoside (DDM) (Glycon) at a concentration of 0.05% was used. Measurements with the samples in detergent solution and in liposomes were carried out in a buffer composed of a mixture of 50 mM bis–tris propane and 50 mM CAPS at pH 9.

2.5. Experiments with fully reduced ba_3 CytcO in nanodiscs

Either a sample containing detergent-solubilized ba_3 oxidase (∼5 μM enzyme in 10 mM Hepes, pH 7.5, 0.05% DDM, 0.5 μM PMS) or nanodisc-reconstituted ba_3 Cyt*c*O (∼5 μM enzyme in 10 mM Hepes, pH 7.5, 0.5 μM PMS) was transferred to a Thunberg cuvette and an amount of Na-ascorbate corresponding to a final concentration of 2 mM was placed in the sidearm of the cuvette. The atmosphere was exchanged for N_2 on a vacuum line and the Cyt*c*O was reduced upon addition of the ascorbate to the enzyme solution. Upon full reduction (as determined from the optical absorption spectrum) of the Cyt*c*O, the atmosphere was exchanged for CO and the sample was allowed to incubate for at least 30 min. Measurements of the reaction of the reduced enzyme with oxygen were performed using a locally modified flow-flash apparatus (Applied Photophysics) as described in [26]. Briefly, the Cyt*c*O

nanodisc preparation (10 mM Hepes, pH 7.5) was rapidly mixed at a ratio of 1:2 with an O_2-saturated solution (100 mM Hepes, pH 7.5) and the reaction was initiated by light-induced displacement of the CO ligand ~30 ms after mixing (10 ns, 200 mJ, 532 nm, Nd:YAG Brilliant B, Quantel). Electron and proton-transfer reactions were monitored at different wavelengths on an oscilloscope. Measurements with the detergent solubilized ba_3 oxidase were performed identically, except that the O_2-saturated solution contained additionally 0.05% DDM. For proton uptake measurements, buffer was removed from the protein samples using a PD-10 column pre-equilibrated with 150 mM KCl, pH ~7.5 (and 0.05% DDM in case of detergent solubilized enzyme). Measurements of proton uptake from solution during oxidation of the ba_3 Cyt*c*O were performed using the pH sensitive dye phenol red as described in [21].

3. Results and discussion

Fig. 1A shows a size-exclusion chromatogram at 280 nm, reporting the total protein content (i.e., both MSP and Cyt*c*O) for nanodiscs composed of soybean lipids containing aa_3 Cyt*c*O (denoted "crude aa_3-nanodiscs"). These Cyt*c*O-containing nanodiscs were obtained using a lipid:MSP:Cyt*c*O molecular ratio of approximately 500:10:1. As seen in the Figure, we observed mainly a single peak with a small contribution of larger fragments (see left-hand side of the peak). The presence of a single peak indicates that the main fraction of the nanodisc preparation was uniform having a well-defined size. The probability of complete reconstitution of all Cyt*c*Os into nanodiscs increases statistically with an increasing MSP:Cyt*c*O ratio. However, an excess MSP also results in formation of empty nanodiscs. The MSP:Cyt*c*O ratio of 10:1 is similar to that used in an earlier study of an ABC transporter with MSP1E3D1 [27] and corresponds to an excess MSP by a factor of 5 because two MSPs are present in each nanodisc.

The lipid:MSP ratio of 100:2 used here is the same as found to be optimal for reconstitution of an ABC transporter [27] and similar to that used for reconstitution of bacteriorhodopsin [28]. A lower lipid:MSP ratio of 70:2 resulted in three peaks in the size-exclusion chromatogram (not shown) reflecting a non-uniform preparation. Previous studies have shown that on average one aa_3-Cyt*c*O from *R. sphaeroides* is reconstituted per liposome [29] and there are no indications that this bacterial Cyt*c*O would require multimerization for function. Consequently, one Cyt*c*O per nanodisc/liposome is sufficient for function.

The collected fractions from gel-filtration experiment were analyzed by measuring the absorbance at 280 nm (total protein content) and at 420 nm (oxidized Cyt*c*O). As shown in Fig. 1B, the elution patterns at these two wavelengths are very similar, indicating co-elution (and thus complex formation) of Cyt*c*O and total protein (i.e. both the MSP and Cyt*c*O) in fractions ~10–13. Furthermore, we prepared a sample containing a fluorescently labeled lipid (TR-DHPE) at a concentration corresponding to one fluorescent lipid molecule per 10 nanodiscs. An analysis of this sample using a fluorescence plate reader showed that the fluorescence signal overlaps with the total protein (A^{280}) as well as the Cyt*c*O spectrum (A^{420}) (Fig. 1B), which further supports our conclusion that the aforementioned fractions contain Cyt*c*O within nanodiscs. It should be noted that the fluorescently-labeled lipids were only used in this experiment to detect co-localization of the nanodisc lipids and Cyt*c*O. The spectroscopic experiments discussed below were performed in the absence of TR-DHPE. The protein composition in the different fractions of the main peak was also verified using SDS PAGE electrophoresis (Fig. 1C). Furthermore, the absorption spectra of the nanodisc-reconstituted Cyt*c*O before gel filtration were compared with the spectra of the protein in the fraction with the highest Cyt*c*O content, number 11, (Fig. 1D). There are no differences, suggesting that the Cyt*c*O-nanodisc preparation prior to gel filtration is substantially homogeneous and can be used for functional studies without the gel filtration step.

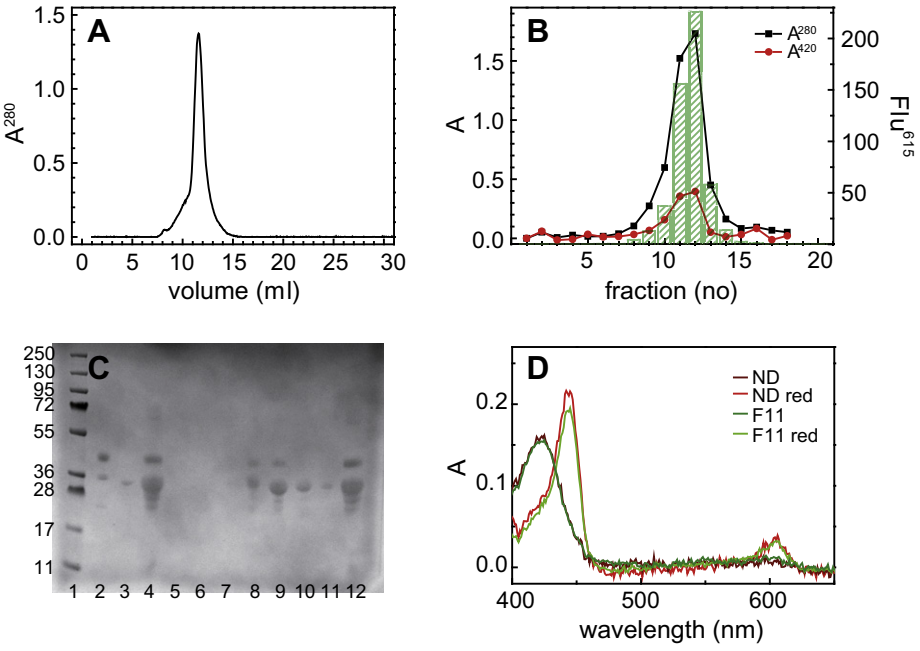

Fig. 1. Reconstitution of aa_3 *R. sphaeroides* Cyt*c*O in soybean lipid nanodiscs. (a) Size-exclusion chromatogram at 280 nm for Cyt*c*O nanodiscs. (b) Analysis of 1 ml fractions from the gel filtration of Cyt*c*O nanodiscs supplemented with fluorescent lipids at a ratio of one fluorescent lipid per 10 nanodiscs. Detection of the total protein content at 280 nm (black squares), absorbance of oxidized Cyt*c*O at 420 nm (red circles) and fluorescence at 610 nm (fractions containing fluorescent lipids, excitation at 584 nm) (green bars). (c) SDS–PAGE where the lanes correspond to: 2 Cyt*c*O (0.1% DDM), 3 MSP, 4 and 12 Cyt*c*O nanodiscs before gel filtration and 5–11 fractions 8–14 (see panel b). (d) Absorption spectra of oxidized (dark colored) and reduced (light colored) Cyt*c*O in nanodiscs before gel filtration (red) and in fraction 11 (green, see panel b), all scaled to 1 μM Cyt*c*O.

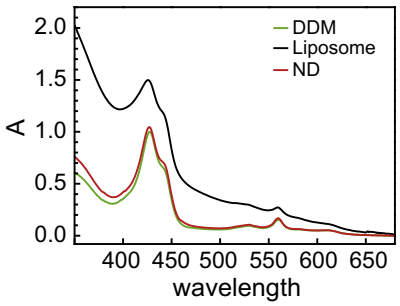

Fig. 2. Absorbance spectra of fully reduced ba_3 CytcO. Shown are the absorption spectra of ba_3 CytcO (in an anaerobic cuvette with 2 mM ascorbate and 0.5 μM PMS) solubilized in detergent solution (DDM), reconstituted in ~50 nm liposomes (SUV) and ~12 nm nanodiscs (ND). Protein concentrations used were ~5 μM, ~4 μM and ~5 μM for DDM, SUV and ND sample, respectively. The amplitudes of the spectra were then normalized to ease comparison.

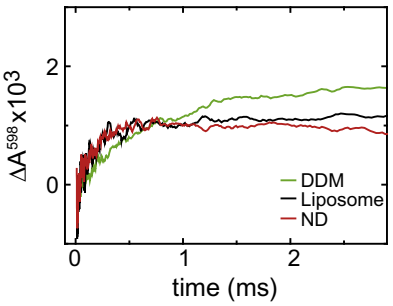

Fig. 3. Proton-coupled electron transfer in aa_3 CytcO. Electron transfer from heme a_3 to heme a is detected as an absorbance increase at 598 nm after flash photolysis of the CO ligand from the two-electron reduced CytcO in 0.05% DDM, soybean liposomes or soybean nanodiscs (ND) at pH 8.9–9. All traces scaled to 1 μM reacting enzyme.

We also reconstituted ba_3 Cyt*c*O from *T. thermophilus* in nanodiscs using the same procedure and compared its optical properties with preparations of the same enzyme in detergent solution and reconstituted into liposomes (Fig. 2). As seen in this figure, the spectra of the nanodisc-reconstituted and detergent-solubilized Cyt*c*Os were approximately the same. In contrast, the spectrum of the liposome preparation is heavily impacted by light scattering (cf. increasing absorbance with decreasing wavelength), illustrating the great advantage of using the nanodiscs over liposomes for optical studies.

The preparation containing aa_3-Cyt*c*O reconstituted in nanodiscs was used for functional studies. Using a flash photolysis set-up allowing microsecond time resolution [26], we followed internal electron transfer, coupled to proton transfer through the K proton pathway [22]. First, the Cyt*c*O was incubated in CO atmosphere under anaerobic conditions. This procedure renders the catalytic site (heme a_3 and Cu_B) reduced with CO bound to heme a_3, while heme a and Cu_A remain oxidized. Because the CO ligand stabilizes the reduced state of heme a_3, laser flash-induced dissociation of the CO ligand results in internal electron transfer from heme a_3 to heme a over a microsecond time scale [30,31]. This electron transfer is followed in time by an additional, slower electron transfer from heme a_3 to heme a, coupled to proton transfer from the catalytic site, from a H_2O molecule [32], through the K pathway with a time constant of 730 μs in detergent solution at pH 9 (cf. [22]). Results from earlier studies showed that the rate of this proton-coupled electron transfer (PCET) accelerates ($\tau \cong 130$ μs) upon incorporation of Cyt*c*O into soybean lipid liposomes. Furthermore, our studies using structural variants of Cyt*c*O in which K pathway residues were modified, indicate that this effect is due to specific interactions between amino acid residues at the Cyt*c*O–membrane interface near the K pathway orifice [22].

In the present study, the same experiments were performed with nanodisc-reconstituted Cyt*c*O (Fig. 3) and compared to the results obtained with Cyt*c*O reconstituted in liposomes or in detergent solution. Here, the absorbance increase at 598 nm reflects internal electron transfer from heme a_3 to heme a, linked to the proton release through the K pathway (the PCET). As depicted in Fig. 3, the PCET in aa_3-nanodiscs at pH ~9 occurred with the same rate as that observed with Cyt*c*O reconstituted in small unilamellar liposomes with a diameter of ~25 nm (for comparison the PCET is also shown with Cyt*c*O in detergent solution). Moreover, the kinetics did not differ between the "crude" aa_3-Cyt*c*O-nanodisc preparation (i.e., no gel filtration) and fraction 11 (cf. Fig. 1B) from the size-exclusion column (data not shown), indicating that removal of the small aggregate fraction preceding the nanodisc peak (cf. Fig. 1A) did not affect the results from these measurements.

As already mentioned above, results from earlier studies have shown that in the aa_3 oxidases proton, transfer through the K-pathway accelerates upon reconstitution into a lipid membrane. The experiments outlined above, where the PCET is investigated in the absence of O_2, make it possible to study this proton transfer time resolved. When a similar two electron reduced sample was prepared with the ba_3 enzyme, no internal electron and proton transfer was observed upon CO dissociation as observed in the aa_3 enzyme. Nonetheless, in the ba_3 Cyt*c*O, proton transfer during reaction of the reduced Cyt*c*O with O_2 occurs through a pathway that is spatially analogous to the K pathway [20]. In the *R. sphaeroides* aa_3 Cyt*c*O, proton transfer during this reaction takes place through the other, D-pathway. Consequently, to compare effects of membrane reconstitution on proton transfer through the analogous pathway (the K pathway) in the aa_3 and ba_3 Cyt*c*Os, we studied different types of reactions in these systems.

The reaction of the reduced nanodisc-reconstituted (using MSP1E3D1, $\varnothing \cong 12$ nm) ba_3 Cyt*c*O with O_2 was investigated and the data were compared to those obtained with ba_3 Cyt*c*O in detergent-solution. The Cyt*c*O was first fully reduced in the presence of CO, which results in formation of the four-electron reduced Cyt*c*O with CO bound to heme a_3. The sample was transferred to one of the syringes of a modified stopped-flow apparatus, while the other syringe was loaded with an O_2-saturated buffer. The two solutions were then rapidly mixed, and after ~30 ms the blocking CO ligand was removed by a laser flash, which allowed O_2 to bind to the reduced heme a_3. Fig. 4 shows absorbance changes at 430 nm during this reaction. These changes are associated with oxidation/reduction of the heme groups, with a major contribution from heme *b*. Following photolysis to remove the CO-ligand (time = 0), the subsequent absorbance changes reflect the oxidation of the enzyme. The data show that for both Cyt*c*O in detergent solution and in nanodiscs, the enzyme became fully oxidized over a time scale of about 2 ms. Yet, significant differences between the data obtained under these different conditions were observed. As seen in Fig. 4A, the amplitude of the kinetic phase with a time constant of ~20 μs, associated with the initial oxidation of heme *b* was apparently larger for the nanodisc-reconstituted Cyt*c*O (qualitatively the same behavior was observed for ba_3 Cyt*c*O in liposomes, data not shown). With the ba_3 Cyt*c*O in detergent solution, this kinetic phase is associated with nearly 100% heme *b* oxidation, which is followed in time by nearly 100% heme *b* re-reduction from Cu_A [21,25,33,34]. Because the 20 μs decrease in absorbance is followed in time by an increase in absorbance (re-reduction of heme *b*) with a time constant of ~80 μs (~60 μs in nanodiscs), the observed amplitude of the absorbance decrease is diminished. In the nanodisc-reconstituted ba_3 Cyt*c*O, the first electron transfer from heme *b* to the catalytic site occurred at the same rate, but

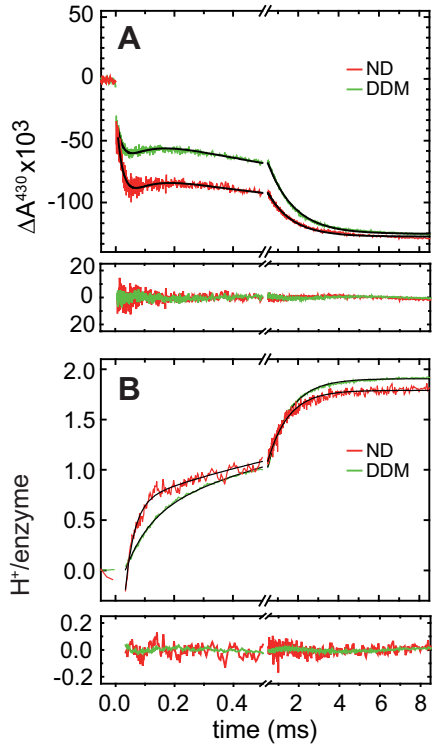

Fig. 4. Reaction of the fully reduced ba_3 Cyt*c*O with oxygen. Shown are the absorbance changes upon photo-dissociation of CO by a laser flash (at $t = 0$) and subsequent reaction of the reduced enzyme with oxygen (DDM, in detergent solution; ND, in nanodiscs). (a) Absorbance changes at 430 nm represent oxidation and reduction of the hemes (with a major contribution of heme *b*). (b) Absorbance changes at 572 nm, of the pH sensitive dye phenol red, associated with pH changes in the surrounding medium caused by proton uptake during oxidation of the Cyt*c*O. The process was biphasic where the rate constant of the faster phase was slower in detergent solution ($\tau \cong 85$ μs) than in nanodiscs ($\tau \cong 35$ μs). The rate of the slower component did not change significantly upon nanodisc reconstitution ($\tau \cong 1.2$ ms). The 572 nm absorbance changes were normalized by HCl titration and are shown converted to protons/enzyme. The traces are differences between those obtained in the absence and presence of buffer (to eliminate contribution from other events then proton uptake at 572 nm). The black lines represent fits of the data with a sum of exponential functions with time constant given in the text. The residuals are shown under each of the graphs.

the Cu_A-heme *b* electron-transfer equilibrium was significantly shifted away from heme *b* (i.e. the heme was not re-reduced to the same extent as in detergent solution) and, therefore, the amplitude of the absorbance decrease was significantly larger. The final oxidation of the Cyt*c*O displayed a time constant of ~1.2 ms (both in nanodiscs and in detergent solution).

Using a pH-sensitive dye in an unbuffered solution, we studied proton-uptake reactions from the aqueous environment during oxidation of the ba_3 oxidase. These proton-uptake reactions are difficult to measure using liposomes for several reasons. On one hand, having two populations with differently oriented enzymes severely complicates the discrimination between the protons that are used as substrate for O_2 reduction and those that are pumped across the membrane. While cumbersome, this drawback might be partially circumvented by using a high concentration of protonophores, rendering the pumped protons invisible. On the other hand, the much higher lipid-to-protein ratio in liposomes drastically increases the buffer capacity of the solution (due to presence of phospholipid head groups) and thus results in a decreased signal in measurements of proton uptake/release reactions. As shown in Fig. 4B, proton uptake through the K pathway analogue could readily be detected in nanodisc-reconstituted enzyme. As with the detergent-solubilized ba_3 Cyt*c*O, two kinetic phases were observed associated with proton uptake from solution. The rate constant of the faster of these processes accelerated from ~85 μs in detergent solution to ~35 μs in nanodiscs. The slower component displayed similar rates for Cyt*c*O in detergent solution and in nanodiscs (~1.2 ms).

As already mentioned above, the nanodisc technology combines the advantage of having the protein in a native-like environment, yet yielding samples that are as optically clear as when having the protein in detergent solution. In recent years, nanodiscs have successfully been used to incorporate and study a range of membrane proteins such as, for example, G protein-coupled receptors [35], rhodopsins [36], ABC transporters [27], F_oF_1-ATP synthase [37] and bacteriorhodopsin [38], opening up new possibilities to study these systems in a membrane environment. In the present study, we have shown that Cyt*c*O from bacterial sources can be reconstituted into nanodiscs. The improved optical properties of such Cyt*c*O-containing nanodiscs, compared to Cyt*c*O-containing liposomes is obvious from Fig. 2. The observed preservation of specific functional properties, which are unique to the presence of the membrane environment of the aa_3 Cyt*c*O reinforces the usefulness of nanodiscs as membrane mimetics. Here, the rate of a PCET through the K-proton pathway, which ends near the protein-membrane interface was significantly accelerated. Furthermore, our study with the ba_3 Cyt*c*O shows that a similar acceleration of proton transport through the K-pathway analogue is observed during the O_2 reaction. In conclusion, the Cyt*c*O-nanodisc system displays the same experimental behavior as Cyt*c*O reconstituted in liposomes and it offers a unique system for optical studies in general and for investigation of effects of interaction partners, which react with the Cyt*c*O surfaces that are exposed to the solvent.

Acknowledgements

These studies were supported by a grant from the Swedish Research Council (to P.B.) and, by grants HL 16101 (to R.B.G) and GM 33775 (to S.G.S.) from the National Institutes of Health. C.v.B. is supported by a fellowship from the Swiss National Science Foundation (SNF).

References

[1] Lee, A.G. (2004) How lipids affect the activities of integral membrane proteins. Biochim. Biophys. Acta 1666, 62–87.
[2] Lee, A.G. (2011) Lipid-protein interactions. Biochem. Soc. Trans. 39, 761–766.
[3] Hunte, C. and Richers, S. (2008) Lipids and membrane protein structures. Curr. Opin. Struct. Biol. 18, 406–411.
[4] Seddon, A.M., Curnow, P. and Booth, P.J. (2004) Membrane proteins, lipids and detergents: Not just a soap opera. Biochim. Biophys. Acta Biomembr. 1666, 105–117.
[5] Bayburt, T.H., Grinkova, Y.V. and Sligar, S.G. (2002) Self-assembly of discoidal phospholipid bilayer nanoparticles with membrane scaffold proteins. Nano Lett. 2, 853–856.
[6] Bayburt, T.H. and Sligar, S.G. (2010) Membrane protein assembly into nanodiscs. FEBS Lett. 584, 1721–1727.
[7] Ritchie, T.K., Grinkova, Y.V., Bayburt, T.H., Denisov, I.G., Zolnerciks, J.K., Atkins, W.M. and Sligar, S.G. (2009) Reconstitution of membrane proteins in phospholipid bilayer nanodiscs. Methods in Enzymology, 211–231 (Chapter 11).
[8] Qin, L., Hiser, C., Mulichak, A., Garavito, R.M. and Ferguson-Miller, S. (2006) Identification of conserved lipid/detergent-binding sites in a high-resolution structure of the membrane protein cytochrome *c* oxidase. Proc. Natl. Acad. Sci. USA 103, 16117–16122.
[9] Svensson-Ek, M., Abramson, J., Larsson, G., Törnroth, S., Brzezinski, P. and Iwata, S. (2002) The X-ray crystal structures of wild-type and EQ(I-286) mutant cytochrome *c* oxidases from *Rhodobacter sphaeroides*. J. Mol. Biol. 321, 329–339.
[10] Liu, J., Qin, L. and Ferguson-Miller, S. (2011) Crystallographic and online spectral evidence for role of conformational change and conserved water in cytochrome oxidase proton pump. Proc. Natl. Acad. Sci. USA 108, 1284–1289.
[11] Soulimane, T., Buse, G., Bourenkov, G.P., Bartunik, H.D., Huber, R. and Than, M.E. (2000) Structure and mechanism of the aberrant ba_3-cytochrome *c* oxidase from *Thermus thermophilus*. EMBO J. 19, 1766–1776.
[12] Luna, V.M., Chen, Y., Fee, J.A. and Stout, C.D. (2008) Crystallographic studies of Xe and Kr binding within the large internal cavity of cytochrome ba_3 from

Thermus thermophilus: Structural analysis and role of oxygen transport channels in the heme-Cu oxidases. Biochemistry 47, 4657–4665.
[13] Liu, B., Chen, Y., Doukov, T., Soltis, S.M., Stout, C.D. and Fee, J.A. (2009) Combined microspectrophotometric and crystallographic examination of chemically reduced and X-ray radiation-reduced forms of cytochrome ba_3 oxidase from *Thermus thermophilus*: structure of the reduced form of the enzyme. Biochemistry 48, 820–826.
[14] Hosler, J.P., Ferguson-Miller, S. and Mills, D.A. (2006) Energy transduction: proton transfer through the respiratory complexes. Annu. Rev. Biochem. 75, 165–187.
[15] Belevich, I. and Verkhovsky, M.I. (2008) Molecular mechanism of proton translocation by cytochrome *c* oxidase. Antioxid. Redox Signal. 10, 1–29.
[16] Ferguson-Miller, S. and Babcock, G.T. (1996) Heme/copper terminal oxidases. Chem. Rev. 96, 2889–2907.
[17] Wikström, M. and Verkhovsky, M.I. (2007) Mechanism and energetics of proton translocation by the respiratory heme-copper oxidases. Biochim. Biophys. Acta (BBA) – Bioenerg. 1767, 1200–1214.
[18] Brzezinski, P. and Gennis, R.B. (2008) Cytochrome c oxidase: exciting progress and remaining mysteries. J. Bioenerg. Biomembr. 40, 521–531.
[19] Kaila, V.R.I., Verkhovsky, M.I. and Wikström, M. (2010) Proton-coupled electron transfer in cytochrome oxidase. Chem. Rev. 110, 7062–7081.
[20] Chang, H.Y., Hemp, J., Chen, Y., Fee, J.A. and Gennis, R.B. (2009) The cytochrome ba_3 oxygen reductase from *Thermus thermophilus* uses a single input channel for proton delivery to the active site and for proton pumping. Proc. Natl. Acad. Sci. USA 106, 16169–16173.
[21] Smirnova, I., Reimann, J., Von Ballmoos, C., Chang, H.Y., Gennis, R.B., Fee, J.A., Brzezinski, P. and Ädelroth, P. (2010) Functional role of Thr-312 and Thr-315 in the proton-transfer pathway in ba_3 cytochrome *c* oxidase from *Thermus thermophilus*. Biochemistry 49, 7033–7039.
[22] Näsvik Öjemyr, L., Lee, H.J., Gennis, R.B. and Brzezinski, P. (2010) Functional interactions between membrane-bound transporters and membranes. Proc. Natl. Acad. Sci. USA 107, 15763–15767.
[23] Qin, L., Mills, D.A., Buhrow, L., Hiser, C. and Ferguson-Miller, S. (2008) A conserved steroid binding site in cytochrome *c* oxidase. Biochemistry 47, 9931–9933.
[24] Mitchell, D.M. and Gennis, R.B. (1995) Rapid purification of wildtype and mutant cytochrome c oxidase from *Rhodobacter sphaeroides* by Ni(2+)-NTA affinity chromatography. FEBS Lett. 368, 148–150.
[25] Von Ballmoos, C., Gennis, R.B., Ädelroth, P. and Brzezinski, P. (2011) Kinetic design of the respiratory oxidases. Proc. Natl. Acad. Sci. USA 108, 11057–11062.
[26] Brändén, M., Sigurdson, H., Namslauer, A., Gennis, R.B., Ädelroth, P. and Brzezinski, P. (2001) On the role of the K-proton transfer pathway in cytochrome c oxidase. Proc. Natl. Acad. Sci. USA 98, 5013–5018.
[27] Alvarez, F.J.D., Orelle, C. and Davidson, A.L. (2010) Functional reconstitution of an ABC transporter in nanodiscs for use in electron paramagnetic resonance spectroscopy. J. Am. Chem. Soc. 132, 9513–9515.
[28] Bayburt, T.H., Grinkova, Y.V. and Sligar, S.G. (2006) Assembly of single bacteriorhodopsin trimers in bilayer nanodiscs. Arch. Biochem. Biophys. 450, 215–222.
[29] Cvetkov, T.L. and Prochaska, L.J. (2007) Biophysical and biochemical characterization of reconstituted and purified *Rhodobacter sphaeroides* cytochrome *c* oxidase in phospholipid vesicles sheds insight into its functional oligomeric structure. Protein Expr. Purif. 56, 189–196.
[30] Verkhovsky, M.I., Jasaitis, A. and Wikström, M. (2001) Ultrafast haem-haem electron transfer in cytochrome *c* oxidase. Biochim. Biophys. Acta – Bioenerg. 1506, 143–146.
[31] Ädelroth, P., Brzezinski, P. and Malmström, B.G. (1995) Internal electron transfer in cytochrome c oxidase from *Rhodobacter sphaeroides*. Biochemistry 34, 2844–2849.
[32] Brändén, M., Namslauer, A., Hansson, Ö., Aasa, R. and Brzezinski, P. (2003) Water-hydroxide exchange reactions at the catalytic site of heme-copper oxidases. Biochemistry 42, 13178–13184.
[33] Siletsky, S.A., Belevich, I., Jasaitis, A., Konstantinov, A.A., Wikström, M., Soulimane, T. and Verkhovsky, M.I. (2007) Time-resolved single-turnover of ba3 oxidase from *Thermus thermophilus*. Biochim. Biophys. Acta 1767, 1383–1392.
[34] Smirnova, I.A., Zaslavsky, D., Fee, J.A., Gennis, R.B. and Brzezinski, P. (2008) Electron and proton transfer in the ba_3 oxidase from *Thermus thermophilus*. J. Bioenerg. Biomembr. 1, 7.
[35] Leitz, A.J., Bayburt, T.H., Barnakov, A.N., Springer, B.A. and Sligar, S.G. (2006) Functional reconstitution of b_2-adrenergic receptors utilizing self-assembling Nanodisc technology. BioTechniques 40, 601–612.
[36] Bayburt, T.H., Leitz, A.J., Xie, G., Oprian, D.D. and Sligar, S.G. (2007) Transducin activation by nanoscale lipid bilayers containing one and two rhodopsins. J. Biol. Chem. 282, 14875–14881.
[37] Ishmukhametov, R., Hornung, T., Spetzler, D. and Frasch, W.D. (2010) Direct observation of stepped proteolipid ring rotation in E. coli $F_o F_1$ -ATP synthase. EMBO Journal. 29, 3911–3923.
[38] Bayburt, T.H. and Sligar, S.G. (2003) Self-assembly of single integral membrane proteins into soluble nanoscale phospholipid bilayers. Protein Sci. 12, 2476–2481.